ORGANOMETALLICS

ARTICLE

pubs.acs.org/Organometallics

Rhenium Nitrosyl Complexes Bearing Large-Bite-Angle Diphosphines

Balz Dudle, Kunjanpillai Rajesh, Olivier Blacque, and Heinz Berke*

Institute of Inorganic Chemistry, University of Zürich, Winterthurerstrasse 190, CH-8057 Zürich, Switzerland

Supporting Information

ABSTRACT: A series of $[ReBr_2(MeCN)(NO)(P\cap P)]$ complexes (P∩P = 1,1′-bis(diphenylphosphino)ferrocene (dppfc) (**1a**), 1,1′-bis(diisopropylphosphino)ferrocene (diprpfc) (**1b**), 2,2′-bis(diphenylphosphino)diphenyl ether (dpephos) (**1c**), 10,11-dihydro-4,5-bis(diphenylphosphino)dibenzo[*b*,*f*]oxepine (homoxantphos) (**1d**), 4,6-bis(diphenylphosphino)-10,10-dimethylphenoxasilin (Sixantphos) (**1e**)) were prepared with diphosphines varying in the P−Re−P bite angles. **1a**,**c**−**e** were obtained from the reaction of $[ReBr_5(NO)][NEt_4]_2$ with an excess of the respective diphosphine in MeCN or MeCN/THF mixtures at elevated temperatures. Compound **1b** was obtained by an alternate route, cleaving the dinuclear $[\{ReBr(\mu_2\text{-}Br)(NO)(diprpfc)\}_2]$ unit (**2b**) with MeCN. **2b** was prepared from the reaction of $[ReBr_5(NO)][NEt_4]_2$ with diprpfc in EtOH. The reaction of **1a**−**d** with $HSiEt_3$ gave the seven-coordinate $[ReBr(H)_2(SiEt_3)(NO)(P\cap P)]$ compounds **4a**−**d**, of which **4a**,**c**,**d** are only stable in solution in the presence of $HSiEt_3$. The $SiMe_3$ (**4f**) and $SiCl_3$ (**4g**) derivatives of **4b** were also prepared by applying the reaction of **1b** with $HSiMe_3$ and $HSiCl_3$. **1a**,**c**,**e**, **2b**, and **4f**,**g** were structurally characterized. For **1c**,**e**, **2b**, and **4f**,**g** NO/Br disorder was observed, which originates from the presence of two isomeric forms in the crystals of the respective compounds. For **1c**,**d** fast interconversion of these isomers could be observed in their $^{31}P\{^1H\}$ NMR spectra at room temperature.

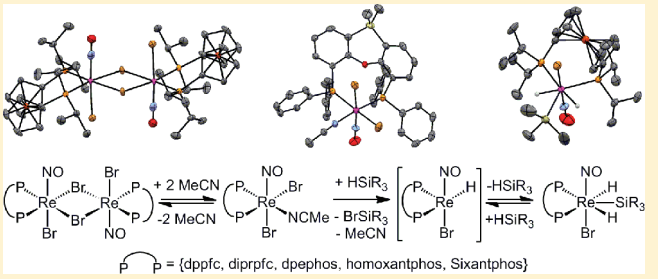

INTRODUCTION

Rhenium indeed possesses substantial affinity for hydrogen so that hydride and dihydrogen ligands are stabilized in compounds with low and high coordination numbers (CN = 5,[1] 6,[2] 7,[3] 8,[4] 9[4]). Rhenium polyhydrides also exist and can be associated with relatively high formal oxidation states of the rhenium centers.[2,4] Often these polyhydrides were seen to be dynamic either by polytopal rearrangements[5] or by dihydride/dihydrogen ligand transformations ($Re(H_2) \leftrightarrows Re(H)_2$) via oxidative addition/reductive elimination equilibria.[6] These latter steps require the ability of rhenium centers to undergo facile Re(n)/Re(n+II) changes. Together with the high affinity of rhenium for olefins[7] and acetylenes,[8] this points to the general disposition of rhenium compounds to enable hydrogenation catalysis.

Catalytic hydrogenation is an important toolkit facet of modern organic synthesis. This area is, however, dominated by homogeneous catalysts based on platinum-group metals.[9] Although these catalysts are as yet unmatched in activity and selectivity, their use is to a certain extent problematic, since they are expensive and too toxic[10] for pharmaceutical applications. Therefore, products have to be freed from these metals to the ppm level[11] and laborious catalyst recycling might be required. New non platinum group element based hydrogenation catalyses are thus sought to be developed. However, for the development of alternative middle-transition-metal catalysts, such as rhenium complexes, we face the difficulty that they possess a low tendency to form 16e or even 14e complexes, an ability required in catalysis for binding and activation of substrates. Catalytic rhenium complexes have therefore to be tuned for ligand lability, which was thought to be accomplishable by ligand effects, such as cis labilization via π donors and the trans influence and trans effect of ligands, via ligands with variable electron counts and the use of large-bite-angle diphosphines.

In our group we systematically approached nitrosyl hydride rhenium chemistry with the NO and H groups as trans effect and trans influence ligands. The Re−NO fragment, in addition, was thought to be especially suited for hydrogenations, since it also is isoelectronic with Ru−CO or Ru−PR_3 and Rh−X fragments, often encountered in hydrogenation[12] and hydroformylation[13] reactions. The idea to mimic ruthenium group chemistry with isoelectronic rhenium fragments initiated developments in $[ReH(X)(L)(NO)(PR_3)_2]$ complexes (X = H, Br; L= labile ligand, R = Cy, *i*-Pr) catalyzing hydrogenations,[14] dehydrogenative silylations,[1] and dehydrogenative aminoborane coupling[15] reactions. An in-depth DFT study of Liu et al. on the hydrogenation with the *trans*-$[Re(H)_2(\eta^2\text{-}C_2H_4)(NO)(PMe_3)_2]$ model system[16] revealed that this fragment would suffer from unfavorable, but crucial stereochemical circumstances appearing during catalysis. The trans-phosphine arrangement[17] is expected to support strong binding of olefin ligands[14] and thus impedes catalytic hydrogenations. We therefore tried to approach

Received: February 1, 2011
Published: May 16, 2011

Scheme 1. Synthetic Access to $[ReBr_2(MeCN)(NO)(P\cap P)]$ Complexes

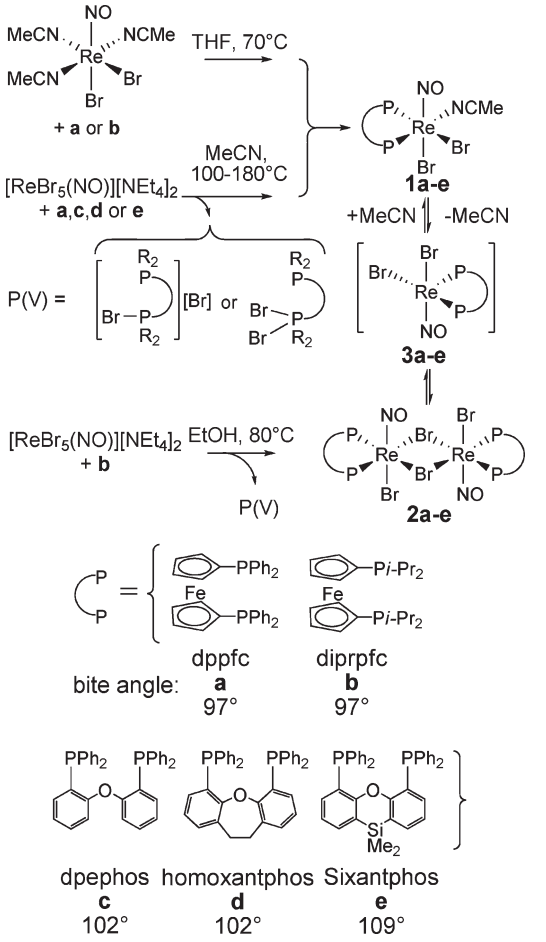

improvement of the potential for catalysis of $[ReH_2(\eta^2\text{-}C_2H_4)(NO)(PR_3)_2]$ systems by changing the coordination pattern from a trans to a cis phosphine arrangement, which we thought to be accomplishable best with chelating diphosphine ligands or even more effectively with $[ReBr_2(MeCN)(NO)(P\cap P)]$ complexes bearing large-bite-angle diphosphines enhancing further the stabilization of 16e species and thus providing promising hydrogenation catalysts.

RESULTS AND DISCUSSION

Preparation of Rhenium Nitrosyl Complexes Bearing Bidentate Large-Bite-Angle Diphosphines. Bidentate diphosphine ligands are characterized in electronic terms by their donicity,[18] in size by their bulk[19] (cone angle at each P center) and by their bite angle.[20] For many catalytic processes it is the state of the art to use large-bite-angle diphosphines, since their catalytic performance often turns out to be superior to that of large-cone-angle monophosphines.[21] The preparation of the large-bite-angle $[ReBr_2(MeCN)(NO)(P\cap P)]$ derivatives was achieved via ligand substitution reactions starting from $[Re^{I}Br_2(MeCN)_3(NO)]$ and $[Re^{II}Br_5(NO)][NEt_4]_2$ compounds developed earlier in our group.[3] It should be noted that attempts to prepare small-bite-angle analogues employing dmpe/dppe or dppm from $[ReBr_2(MeCN)_3(NO)]$ or $[ReBr_5(NO)][NEt_4]_2$ failed. This could be interpreted in terms of $[ReBr_2(MeCN)(NO)(P\cap P)]$ complexes being stable only with large-bite-angle diphosphines. Consequently we employed dpephos, homoxantphos, and Sixantphos from van Leeuwen's large-bite-angle 2,2′-bis(diphenylphosphino)phenyl ether ligand series[21] (Scheme 1). While the bite angle of the bidentate phosphine in this series was varied, the donicity of the ligand was kept approximately constant. In contrast to the known substitution reactions with monodentate phosphine ligands,[14] only moderate to low yields were obtained in the substitution processes of $[ReBr_2(MeCN)_3(NO)]$, with the ferrocenyl diphosphines forming the complexes $[ReBr_2(MeCN)(NO)(dppfc)]$ (**1a**, 63%) and $[ReBr_2(MeCN)(NO)(diprpfc)]$ (**1b**, 31%). Following the synthetic route to the $[ReBr_2(\eta^2\text{-}H_2)(NO)(PR_3)_2]$ (R = *i*-Pr, Cy) species,[3] we attempted also to employ $[ReBr_5(NO)][NEt_4]_2$ as a starting material, reacting it with an excess of dppfc or diprpfc in ethanol at 80−85 °C. According to Scheme 1 the combined ligand substitution and reduction of the rhenium center to concomitantly form P(+V) compounds of the type $[PR_3Br]Br$ or $[PR_3Br_2]$[22] worked better only with the diprpfc ligand, furnishing the dinuclear μ_2-Br substitution product $[\{ReBr(\mu_2\text{-}Br)(NO)(diprpfc)\}_2]$ (**2b**) in 78% yield. An X-ray diffraction study revealed the dinuclear structure of **2b** with trans NO and Br ligands and cis $P_{diphosphine}$ atoms (Figure 1). No NMR spectra of **2b** could be recorded, due to the low solubility of **2b** in noncoordinating solvents.

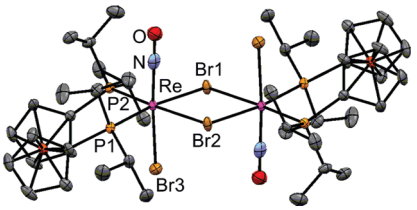

Figure 1. ORTEP diagram of **2b(down)**, with ellipsoids drawn at the 50% probability level. Solvent molecules, H atoms, and NO/Br disorder are omitted for clarity. Selected bond lengths (Å): Br1−Re = 2.6457(5), Br2−Re = 2.6493(5), Br3−Re = 2.5694(6), N−Re = 1.776(5), N−O = 1.124(7), P1−Re = 2.4150(13), P2−Re = 2.4384(14). Selected bond angles (deg): Br1−Re−Br2 = 80.205(19), Br1−Re−P1 = 170.95(3), Br1−Re−P2 = 90.81(3), Br2−Re−P1 = 91.03(3), Br2−Re−P2 = 170.68(3), Br3−Re−N = 175.95(14), O1−N1−Re = 179.4(6), P1−Re−P2 = 97.84(4).

Stirring **2b** at room temperature in a DCM/MeCN mixture resulted in the splitting of the μ_2-Br bridges with quantitative formation of the MeCN complex **1b**. The reaction of $[ReBr_5(NO)][NEt_4]_2$ with an excess of dppfc in a 7:3 mixture of MeCN and THF furnished the direct formation of **1a** in 74% yield based on the $[Re^{II}Br_5(NO)][NEt_4]_2$ starting material (Scheme 1). In this reaction again the diphosphine served as a ligand, as well as a reducing agent of the Re(+II) center producing P(+V) compounds, which was indicated by the appearance of additional signals in the $^{31}P\{^1H\}$ NMR spectra of the reaction solutions. This facile access to **1a**,**b** prompted us to try also the preparation of other structurally related complexes bearing large-bite-angle diphosphines. Unlike the ferrocene-based ligands, dpephos (**c**), homoxantphos (**d**) and Sixantphos (**e**) were found to withstand temperatures of 180−200 °C. In this range of temperatures the ligands, as well as the $[ReBr_5(NO)][NEt_4]_2$ salt, became soluble in MeCN and the combined redox and substitution reactions according to Scheme 1 went to completion within 3−5 h with moderate to high yields producing the desired Re(+I) substitution products

dx.doi.org/10.1021/om200092y |*Organometallics* 2011, 30, 2986–2992

Scheme 2. General Sketch of Isomerism in [ReXYBr(NO)(P∩P)] Complexes

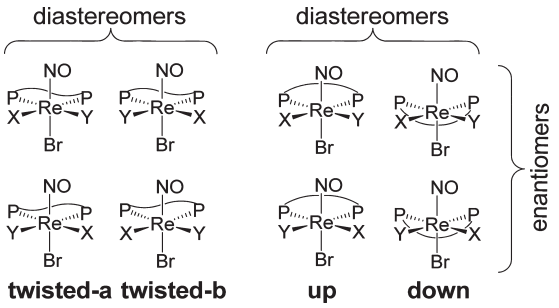

Scheme 3. Mono- and Dinuclear Racemization Pathways of 1a−e for the Br/MeCN Exchange and Virtual Exchange of the Diphosphine Sides

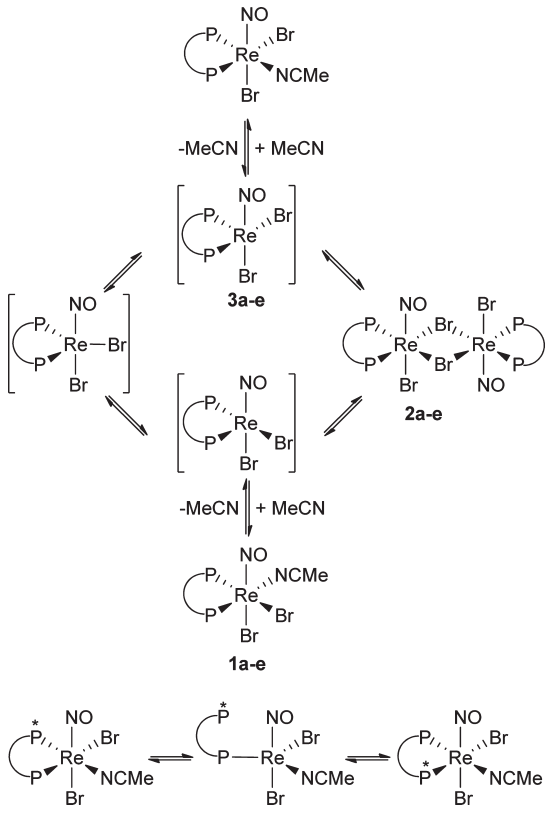

[$ReBr_2$(MeCN)(NO)(dpephos)] (**1c**; 88%), [$ReBr_2$(MeCN)(NO)(homoxantphos)] (**1d**; 72%), and [$ReBr_2$(MeCN)(NO)(Sixantphos)] (**1e**; 56%). For octahedral complexes bearing a rigid bidentate ligand various constitutional and conformational isomers are expected to exist.[23] However, since the trans arrangement of the NO and one Br ligand is favored due to a stabilizing strong "push−pull" π-interaction, the cis position of the diphosphines with respect to the NO/Br axis became enforced by the given electronic conditions.[24] Consequently the other two ligands MeCN and Br had to arrange trans to the $P_{diphosphine}$ atoms. Therefore, only one type of constitutional isomer of **1c−e** could be formed possessing a chiral rhenium center. The backbone of such rigid large-bite-angle diphosphine

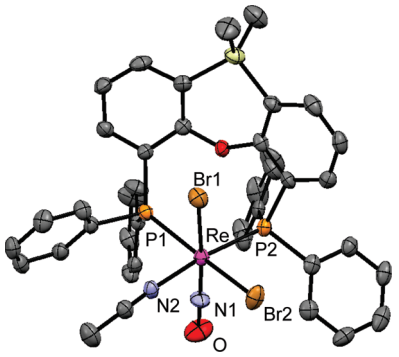

Figure 2. ORTEP diagram of **1e(down)**, with ellipsoids drawn at the 50% probability level. Solvent molecules, H atoms, and NO/Br disorder are omitted for clarity. Selected bond lengths (Å): Br1−Re = 2.5591(6), Br2−Re = 2.6090(5), N1−Re = 1.716(5), N1−O1 = 1.290(6), N2−Re = 2.125(3), P1−Re = 2.4434(10), P2−Re = 2.4049(10). Selected bond angles (deg): Br1−Re−N1 = 174.75(13), Br2−Re−P1 = 167.78(3), Br2−Re−P2 = 89.40(3), N2−Re−P1 = 89.53(8), N2−Re−P2 = 173.27(8), O1−N1−Re = 179(2), N2−Re−Br2 = 84.47(8), P1−Re−P2 = 97.00(3).

ligands could by no means be forced into the P−Re−P plane. Therefore, the backbone of these ligands adopt either an "**up**"/"**down**" or "**twisted-a**"/"**twisted-b**" conformation. This could result theoretically in four enantiomeric pairs of diastereomers/conformers as depicted in Scheme 2. **Up**, **down**, and **twisted** denote the relative positions of the ligand backbone with respect to the NO/Br axis, while **twisted-a**/**twisted-b** would denote the arrangement of the X/Y ligands. The question arises, which isomers are formed, and whether there is a substantial barrier for their interconversions. Such diastereomer interconversions and racemizations between **up**/**down**, respectively, and **twisted-a**/**twisted-b** diastereomers could principally occur via the inversion of the ligand backbone and/or on/off reactions and shift of the rhenium bound leg of the diphosphine to the other side (Scheme 3). It is noteworthy that a mechanism which interconverts **up** into **down** diastereomers would also racemize the **twisted** isomers and vice versa. Inversions of the free ligand backbones seemed more probable for the free diprpfc, dppfc, and dpephos ligands but not necessarily for the bound form in the complexes. The existence of bromide-bridged dimers of type **2** and the observed dynamics in the NMR spectra (vide infra) indicated that isomerization/racemization processes via MeCN dissociation are ongoing reactions in solution at ambient temperatures.

The complexes **1a,c,e** were characterized by X-ray diffraction studies. The ORTEP drawing of **1e** shows a representative example of type **1** complexes (Figure 2). As expected, **1e** possesses a distorted-octahedral structure with a trans NO/Br axis and a cis diphosphine arrangement with respect to this axis. The bond lengths were found to be in the range of typical Br−Re, MeCN−Re, P−Re, and Re−NO bonds. However, the large-bite-angle diphosphine causes steric congestion in the P−Re−P plane, which is reflected in the compression of the N2−Re−Br2 angle down to 84.47(8)°. Except for **1a**, the structures of all complexes showed NO/Br disorder at varying ratios of the diastereomers. **1c,e** and **2b** crystallize as mixtures of the **up** and **down** diastereomers (**up**, **1c** 10%, **1e** 14%, **2b** 8%; **down**, **1c** 90%, **1e** 86%, **2b** 92%), while **1a** and **4e,f** (vide infra) crystallize in the **twisted** form (**twisted-a**, **1a** 0%, **4e** 47%, **4f** 38%; **twisted-b**, **1a** 100%, **4e** 53%, **4f** 62%). The preference for **up** or **down** isomers

seemed to be governed by steric factors. Generally the **down** conformations are favored apparently avoiding van der Waals contacts of the Br ligand with one of the diphosphine phenyl groups with the closest Br···H_{Ph} significantly below the typical distance[25] of 2.95 Å. This effect causes a slight tilting of the NO/Br axis in the **up** isomers. However, the X-ray studies of **1a**,**c**,**e** and **2b** revealed that the orientation of the NO/Br axis with respect to the ligand backbone has otherwise only minor influence on the overall structural features of these complexes. The X-ray studies allowed also to determine the P−Re−P angles, which were found to be quite similar for all the structurally investigated derivatives: **1a** (98.90(3)°), **1c** (100.79(4)°), and **1e** (97.00(3)°), despite the fact that dppfc (97°), dpephos and homxantphos (102°), and Sixanphos (109°) possess substantially different natural bite angles.[20,21] To explain this discrepancy, one has to take into account that the quoted natural bite angles[20] are determined by molecular dynamic simulations with a standard-type P−M distance of 2.3 Å. Since the actual Re−P distances in **1a**−**e** are about 2.45 Å, the natural bite angles are systematically too low for rhenium complexes. The "corrected natural bite angles" would thus be 89° (dppfc, diprpfc), 95° (dpephos, homoxantphos), and 100° (Sixantphos). Even if one took these corrected values as the reference values, we would still be left with deviations, which presumably originate on the one hand from a high degree of conformational flexibility of the diphosphine backbones and on the other hand from thermodynamically very strong Re−P bonds, for which an optimal orbital overlap between the phosphorus atoms and the rhenium center is crucial. Thus, the optimization of the Re−P orbital overlaps outweighs the deformation energies of the ligand backbones.

The IR spectra of **1a**−**e** each displayed a single characteristic ν(NO) band in the range of 1680−1700 cm^{-1}. The ^{1}H NMR spectra of **1a**−**e** consisted of broadened signals for the diphosphine and the MeCN ligands in a 1:1 ratio. For **1d**,**e** broad and overlapping signals for bound and free MeCN were observed, which points to the presence of dissociation equilibria at room temperature, while for **1a**−**c** one signal for a rhenium-bound MeCN was visible. The ^{31}P{^{1}H} NMR spectra of compounds **1a**−**e** consisted of two broad resonances (1:1 integration ratio), for which no coupling patterns were resolved. However, in the case of **1c**,**e** an additional ^{31}P{^{1}H} NMR signal became observable, which disappeared upon addition of MeCN. We interpreted this in terms of a dissociation equilibrium of the MeCN complexes **1d** and **1e** forming the μ_2-Br dimers **2d**,**e** (Scheme 3). Presumably the MeCN dissociation is promoted by "steric pressure" imposed on this ligand by the large-bite-angle diphosphines. The broadness of the ^{1}H and the ^{31}P{^{1}H} NMR spectra and the absence of the expected coupling pattern of the ^{31}P{^{1}H} NMR signals can be explained by assuming dynamics with exchange of the inequivalent ^{31}P nuclei at a rate in the range of the NMR time scale. This exchange might proceed via either formation of μ_2-Br intermediates (**2a**−**e**), which are assumed to be cleaved randomly, or via the formation of a transient unsaturated trigonal-bipyramidal intermediate, which can rebind the freed MeCN at both sides of the Br ligand with equal probability (Scheme 3).

Both types of rearrangements of the upper part of Scheme 3 lead to racemization of **1a**−**e**. An alternative genuine P atom exchange mechanism would involve dissociation of one "leg" of the diphosphine followed by a combined shift and rotation of the remaining Re−P bond, as depicted at the bottom of Scheme 3.

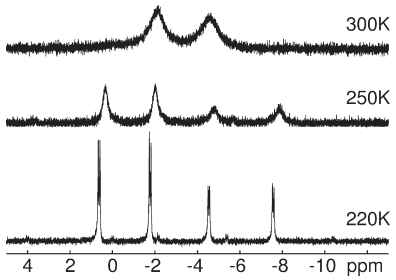

Figure 3. ^{31}P{^{1}H} NMR spectra of **1c** at various temperatures ($CDCl_3$, 162 MHz).

However, the acetonitrile dissociation pathway looks more plausible to occur than the genuine P atom exchange of the diphosphine, since only acetonitrile dissociation could lead to strongly broadened NMR signals for MeCN (bound and free).

To gain further insight into the dynamics, we recorded the ^{31}P{^{1}H} spectra of **1a** and **1c**−**e** at low temperature, thus slowing down the exchange processes. In the case of the dppfc complex **1a** the broad signals observed at room temperature sharpened indeed into a pair of doublets at 6.83 and 0.37 ($^2J_{PP}$ = 13 Hz) ppm - ($CDCl_3$, 240 K, 162 MHz). In contrast to the spectrum of **1a**, the two broad signals observed in the room-temperature spectrum of the dpephos derivative **1c** turned out to be coalescing signals of two species, each giving rise to a set of two doublets at 0.54 and −1.84 ($^2J_{PP}$ = 12 Hz) and at 4.61 and −7.66 ($^2J_{PP}$ = 11 Hz) ppm ($CDCl_3$, 220 K, 162 MHz, Figure 3). At 220 K the ^{31}P{^{1}H} NMR signals of **1d** remained broad, providing no further information on the involved dynamic processes. The room-temperature spectrum of a solution of **1e** in $CDCl_3$ consisted of two broad signals at 1.0 and −4.0 ppm assigned to **1e** and a sharp signal at 26.1 ppm assigned to **2e**. Warming the sample to 320 K leads to a significant broadening of the signal of **2e** at 26.1 ppm. At the same time the two signals of **1e** collapsed into a coalescing signal at −5.2 ppm. Cooling a sample of **1e** to 240 K led to a sharp signal for **2e** at 26.0 ppm (0.08 P) and to four sets of doublets for **1e** at 4.7 and 0.1 ppm (0.10 P), at 0.3 and −3.4 ppm ($^2J_{PP}$ = 10 Hz, 0.66 P), at −3.7 and −11.4 ppm (0.04 P), and at −7.2 and −14.1 ppm (0.12 P). From these results we can conclude that at least in the case of **1c**,**e** different conformers are present in solution (Figure 3). In the case of **1c** the ^{31}P{^{1}H} NMR signals are attributed to the **1c(up)** and **1c(down)** conformers and in the case of the spectrum of **1e** four conformers are distinguishable with prevailing amounts of **1e(down)**, which would be in accord with the results of the crystallographic analysis of **1e** (vide supra). Minor signals were assigned to **1e(up)**, **1e(twisted-a)**, and **1e-(twisted-b)** (Scheme 2). At room temperature these conformers are in fast exchange on the NMR time scale. An additional exchange is observed between **1e** and **2e** at elevated temperatures, indicating that the isomerization pathway via the μ_2-Br dimers is operative at least in this case (Scheme 3). In the cases of **1a**,**d**, for which only one set of doublets or very broad signals could be detected, we can neither confirm nor exclude the presence of more than one conformer in solution, since the NMR spectra of these diastereomers could be similar and practically indistinguishable.

Preparation of the Hydride Complexes 3a−f. On the basis of the well-established hydride chemistry of [ReH(η^2-BH_4)-(NO)(PR_3)$_2$] complexes (R = Cy, *i*-Pr, *p*-tolyl)[3,14] with trans monodentate phosphines, we attempted the transformation of **1a**−**e** into the related rhenium hydride complexes applying

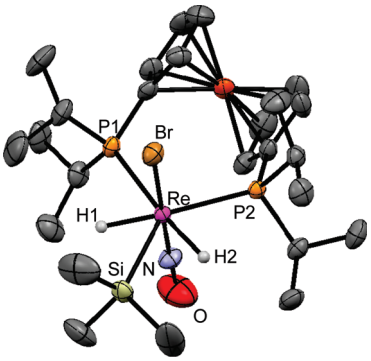

Figure 4. ORTEP diagram of **4f(twisted)** with the ellipsoids drawn at 50% probability. NO/Br disorder and H atoms are omitted for clarity. Selected bond lengths (Å): Br1−Re = 2.5413(12), H1−Re = 1.66, H1−Re = 1.59, N−O = 1.309(10), N−Re = 1.744(8), P1−Re = 2.5271(7), P2−Re = 2.5051(7), Re−Si = 2.5202(8). Selected bond angles (deg): Br1−Re−N = 176.67(17), H1−Re−P2 = 73, H1−Re−P1 = 69, N−O−Re = 178.6(9), P1−Re−P2 = 102.36(2), P1−Re−Si = 131.70(3), P2−Re−Si = 125.63(3).

hydride reagents, such as $[NBu_4][BH_4]$, $LiAlH_4$, KH, and KH/18-crown-6 in THF. Despite extensive variations of the reaction temperatures and of the stoichiometries of the reactants, we found the course of any of these reactions ending up in inseparable mixtures of compounds. However, when $HSiEt_3$ was used as a hydride source to react with **1a**−**d**, the dihydride silyl complexes $[ReBr(H)_2(SiEt_3)(NO)(P\cap P)]$ (**4a**−**d**) were formed smoothly, for which we propose a pentagonal-bipyramidal structure with the hydrides, the silyl moiety, and the diphosphine in the pentagonal plane, in close analogy to the structurally fully characterized **4f** (Figure 4, vide infra). The analogous reaction with **4e** still furnished a mixture of products, which could not be separated. We suppose that at least one of the products has a silyl dihydride structure related to **4f**. **4a**,**c**,**d** were found to be stable in solution, but only in the presence of the silane. These species were therefore characterized via their NMR and IR spectra in solution, which were in the hydride part similar to that of the stable **4f** complex. Attempts to isolate **4a**,**c**,**d** led to the formation of brick red precipitates, from which we concluded that **4a**,**c**,**d** are in equilibrium with the 16e complex $[ReBrH(NO)(P\cap P)]$ (**5a**−**d**) and $HSiEt_3$ according to Scheme 4, which subsequently may oligomerize to μ_2-H dimers, trimers, or even higher oligomers composed of **5a**−**d** units occurring already at low concentrations of the free intermediates **5a**−**d**. Similar oligomerizations of isoelectronic intermediates were reported to be formed with Crabtree's $[Ir(diene)(PCy_3)(pyridine)][PF_6]$ catalysts in the presence of H_2[26] or the $[Re(H)_7(PPh_3)_2]$ complex at elevated temperatures.[4] In contrast to this observation for **1a**,**c**,**d**, complex **1b** bearing the more electron donating diprpfc ligand reacted with $HSiEt_3$, forming a stable seven-coordinate $[ReBr(H)_2(SiEt_3)(NO)(diprpfc)]$ (**4b**) complex. Because of the liquid nature of **4b**, which therefore could not be characterized by a X-ray diffraction study, the $SiMe_3$ derivative **4f** was also prepared and obtained in 92% yield by applying $HSiMe_3$ and was studied by X-ray diffraction (Figure 4). As expected, the NO and Br ligands are trans and the P atoms cis. The $SiMe_3$ moiety lies in the P−Re−P plane, forming a triangle with the diprpfc P atoms (selected angles (deg): P1−Re−P2 = 102.36(2), P1−Re−Si = 131.70(3), P2−Re−Si = 125.63(3)). The two hydrides were located and refined in this plane between the P and Si atoms. The P−Re and

Scheme 4. Reaction of 1a−d with $HSiEt_3$

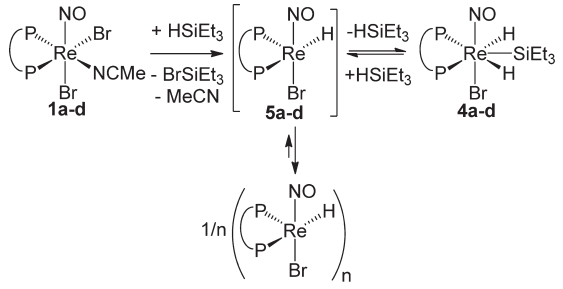

Si−Re bonds are 2.50−2.55 Å, somewhat longer than the Re−P bonds (about 2.45 Å) in the type **1** complexes, but still in the range of typical Re−P single bonds. The NO−Re−Br axis remains largely unaffected by the change from type **2b** to type **4b** complexes, showing only minor differences in the Re−NO (**4b**, 1.744(8) Å; **2b**, 1.776(5) Å) and the NO bond (**4b**, 1.309(10) Å; **2b**, 1.124(7) Å), which may originate from somewhat stronger back-bonding in **4a**. This is also reflected in the IR spectra of **4b** (ν(NO) 1693 cm^{-1}) and **2b** (ν(NO) 1681 cm^{-1}). Furthermore, a NO/Br disorder clearly demonstrates the presence of **twisted-a** and **twisted-b** diastereomers formed in a 47:53 ratio (Scheme 2). Since the discrimination between these **twisted-a** and **twisted-b** species arises from the asymmetry introduced by the SiR_3 moiety, the interconversion of these species is expected to be very fast, on the basis of reversible $HSiMe_3$ loss and readdition or/and rotation of the $SiMe_3$ moiety. Therefore, it is not surprising that neither the ^1H and $^{31}P\{^1H\}$ NMR nor the IR spectra of **4a**−**d** point to the presence of more than one conformer. To probe the influence of the silicon substituents, the $SiCl_3$ derivative **4g** was prepared via the reaction of **1b** with $HSiCl_3$. The formation of **4g** was accompanied by a partial bromide/chloride exchange, yielding a mixture of products. Since this mixture could not be separated, $[NEt_4]Cl$ was added to the reaction solution to achieve a quantitative Cl/Br exchange. Chromatographic workup yielded pure **4g** (66%). In order to compare the structures of **4g**,**f**, an X-ray diffraction study on single crystals of **4g** was carried out. On the basis of the π-acceptor property of the $SiCl_3$ moiety, the Si−Re distance in **4g** (2.3948(6) Å) was found to be significantly shorter than that of **4f** (2.5202(8) Å). This is reflected in the ν(NO) bands of **4f** (1678 cm^{-1}) and **4g** (1718 cm^{-1}). From these observations we concluded that electronic substituent effects of silyl ligands are similar to those of respective phosphorus ligand series.[18] Moreover, the significantly shorter Re−Si bond in **4g** indicates a drastically increased bond strength.

CONCLUSION

This work established an efficient and versatile synthetic approach to $[ReBr_2(MeCN)(NO)(P\cap P)]$ complexes bearing the large-bite-angle diphosphines dppfc, diprpfc, dpephos, homoxantphos, and Sixantphos. X-ray diffraction studies revealed that these compounds can form backbone isomers of the type **up**, **down**, and **twisted**, as confirmed by exemplary X-ray structures. However, in the NMR and IR spectra of these compounds, the interconversion of such isomers could not be pursued quantitatively, preventing the assessment of relative stabilities of these isomers in solution. The large-bite-angle diphosphine rhenium nitrosyl chemistry seemed to be dominated by the relative stability

of the 16e intermediates of types **3** and **5** triggered supposedly mainly by the large-bite-angle effect of the diphosphines, in addition to the π-push−pull effect of the NO/Br axis as a stabilizing factor. If they are indeed long-lived enough, type **3** and **5** intermediates could take over roles in important catalytic reactions, otherwise accomplishable only with platinum-group-metal centers.

EXPERIMENTAL SECTION

General Considerations. All manipulations were carried out under an atmosphere of dry nitrogen using either standard Schlenk techniques or an M. Braun glovebox. All solvents were dried, distilled, and degassed according to standard laboratory procedures. The diphosphine ligands $[ReBr_5(NO)][NEt_4]_2$ and $[ReBr_2(MeCN)_3(NO)]$ were prepared according to published methods.[3,14,21,27] NMR spectra were recorded on a Bruker AV-2 500 spectrometer. Chemical shifts are expressed in parts per million (ppm) and referenced to the solvent's residual signals[28] or in the case of $^{31}P\{^1H\}$ NMR spectra to the external standard 85% H_3PO_4 at δ 0.0 ppm. IR spectra were recorded on a BioRad Excalibur spectrometer. Microanalyses were carried out at the Anorganisch-Chemisches Institut of the University of Zürich.

Crystal Structure Determination. Relevant details about the structure refinements are given in the Supporting Information. Crystallographic data have been deposited with the Cambridge Crystallographic Data Center as CCDC 787668−78772 and 805674. These data can be obtained free of charge from The Cambridge Crystallographic Data Centre via www.ccdc.cam.ac.uk/data_request/cif and are also available as Supporting Information.

[$ReBr_2$(MeCN)(NO)(dppfc)] (1a). *Method 1.* A suspension of $[ReBr_2(MeCN)_2(NO)(THF)]\cdot 2THF$ (0.240 g, 0.356 mmol) and dppfc (0.224 g, 0.404 mmol) in THF (10 mL) was stirred for 5 h at 60 °C. The resulting precipitate was filtered off, washed with a minimum of THF, and dried in vacuo, yielding **1a**·THF (0.250 g, 0.239 mmol, 63%).

Method 2. A mixture of $[ReBr_5(NO)][NEt_4]_2$ (1.003 g, 1.1 mmol) and dppfc (1.000 g, 2.3 mmol) in THF (3 mL) and MeCN (7 mL) was stirred for 12 h at 80 °C. The solution was filtered hot, and the product was allowed to crystallize overnight before it was filtered off and washed with EtOH (3 × 3 mL). After drying in vacuo bright yellow crystals of **1a**·THF were obtained (0.910 g, 0.8 mmol, 74%).

IR (cm^{-1}, KBr pellet): 1685 (s, ν(NO)). ^1H NMR (500 MHz, $CDCl_3$, 27 °C): δ 8.09 (m, 2 H, phenyl), 7.00 (m, 2 H, phenyl), 7.53 (m, 4 H, phenyl), 7.43 (s, 4 H, phenyl), 7.32 (m, 8 H, phenyl), 5.82 (s, 1 H, cp), 4.50 (s, 1 H, cp), 4.44 (s, 1 H, cp), 4.38 (s, 1 H, cp), 4.24 (s, 1 H, cp), 4.22 (s, 2 H, cp), 3.91 (s, 1 H, cp), 2.24 ppm (s, 3 H, MeCN). $^{31}P\{^1H\}$ NMR (202 MHz, $CDCl_3$, 27 °C): δ 4.95 (s broad, 1 P), −0.71 ppm (s broad, 1P). Anal. Calcd for $C_{40}H_{39}Br_2FeN_2O_2P_2Re$ (1043.56 g mol^{-1}): C, 46.04; H, 3.77; N, 2.68. Found: C, 46.00; H, 3.75; N, 2.59.

[$ReBr_2$(MeCN)(NO)(diprpfc)] (1b). *Method 1.* A suspension of $[ReBr_2(MeCN)_2(NO)(THF)]\cdot 2THF$ (0.100 g, 0.148 mmol) and diprpfc (0.068 g, 0.162 mmol) in THF (5 mL) was stirred for 5 h at 60 °C. The precipitate was filtered off, washed with a minimum of THF, and dried in vacuo, yielding **1b** as a yellow powder (0.044 g, 0.053 mmol, 32%).

Method 2. A mixture of **2b** (0.300 g, 0.38 mmol), CH_2Cl_2 (10 mL) and MeCN (1 mL) was stirred for 4 h. During this time the solid **2b** dissolved completely. The solvents were removed in vacuo, and **1b** was obtained quantitatively.

IR (cm^{-1}, KBr pellet): 1683 (s, ν(NO)). ^1H NMR (500 MHz, $CDCl_3$, 27 °C): δ 4.886 (s, 1 H, cp), 4.588 (s, 1 H, cp), 4.392 (s, 1 H, cp), 4.371 (s, 4 H, cp), 4.274 (s, 1 H, cp), 3.719 (s, 1 H, *i*-Pr C*H*$(CH_3)_2$), 3.199 (s, 1 H, *i*-Pr C*H*$(CH_3)_2$), 3.007 (s, 1 H, *i*-Pr C*H*$(CH_3)_2$), 2.769 (m, 4 H, *i*-Pr C*H*$(CH_3)_2$ and MeCN), 1.633−1.102 ppm (m, 24 H, *i*-Pr CH$(CH_3)_2$). $^{31}P\{^1H\}$ NMR (202 MHz, $CDCl_3$, 28 °C): δ 2.27 (s, broad), 0.86 ppm (s, broad). Anal. Calcd for $C_{24}H_{39}Br_2FeN_2OP_2Re$ (835.39 g mol^{-1}): C, 34.51; H, 4.71; N, 3.35. Found: C, 34.33; H, 4.63; N, 3.19.

[$ReBr_2$(MeCN)(NO)(dpephos)] (1c). A suspension of $[ReBr_5(NO)][NEt_4]_2$ (1.000 g, 1.14 mmol) and dpephos (1.000 g, 1.85 mmol) in MeCN (10 mL) was stirred for 3 h at 180 °C in a Büchi pressure tube (*caution*! pressure rises to 4−5 bar). The reaction mixture was allowed to stand for 16 h at room temperature before the product was filtered off, washed with EtOH (3 × 3 mL), and dried in vacuo to yield orange crystalline **1c** (0.960 g, 0.90 mmol, 88%).

IR (KBr pellet, cm^{-1}): 1693 (s, ν(NO)). ^1H NMR (500 MHz, $CDCl_3$, 28 °C): δ 8.1−7.1 (overlapping multiplets, 1 H, dpephos H), 6.84 (s, 1 H, dpephos H), 6.72 (s, 1 H, dpephos H), 6.63 (s, 1 H, dpephos H), 6.02 (s, 1 H, dpephos, H), 2.07 (s, 3 H, MeCN) ppm. $^{31}P\{^1H\}$ NMR (125 MHz, THF-d_8, 28 °C): δ −2.8 (s broad, 1 P), −5.0 (s broad, 1 P) ppm. Anal. Calcd for $C_{38}H_{31}Br_4N_2O_2P_2Re$ (955.63): C, 47.63; H, 3.27; N, 2.93. Found: C, 47.63; H, 3.22; N, 2.97.

[$ReBr_2$(MeCN)(NO)(homoxantphos)] (1d). A mixture of $[ReBr_5(NO)][NEt_4]_2$ (1.000 g, 1.14 mmol) and homoxantphos (1.000 g, 1.77 mmol) in MeCN (10 mL) was stirred for 5 h at 180 °C in a Büchi pressure tube (*caution*! pressure rises to 4−5 bar). The mixture was allowed to stand for 16 h at room temperature before the product was filtered off, washed with EtOH (3 × 3 mL), and dried in vacuo to yield **1d** as an orange microcrystalline solid (0.810 g, 0.83 mmol, 72%).

IR (cm^{-1}, KBr pellet): 1680 (s, ν(NO)). ^1H NMR (500 MHz, $CDCl_3$, 28 °C): δ 8.0−6.8 (overlapping multiplets, 28 H, arom H), 3.2−2.9 (broad multiplets, 4 H, ethylene bridge), 2.2−1.9 ppm (broad, 3 H, MeCN). $^{31}P\{^1H\}$ NMR (125 MHz, THF-d_8, 28 °C): δ 25.3 (s, broad), 1.2 (s broad), −0.3 (s broad) ppm. Anal. Calcd for $C_{40}H_{33}B_2N_2O_2P_2Re$ (981.66): C, 48.94; H, 3.39; N, 2.85. Found: C, 48.69; H, 3.58; N, 2.97.

[$ReBr_2$(MeCN)(NO)(Sixantphos)] (1e). A suspension of $[ReBr_5(NO)][NEt_4]_2$ (1.00 g, 1.14 mmol) and Sixantphos (0.82 g, 1.38 mmol) in MeCN (12 mL) was stirred for 4 h at 200 °C in a Büchi pressure tube (*caution*! pressure rises to 4−5 bar). After it was cooled to room temperature, the yellow solid was filtered off, washed with MeCN (2 × 4 mL), and dried in vacuo to yield **1e** as a yellow solid (0.65 g, 0.64 mmol, 56%).

IR (KBr pellet, cm^{-1}): 1680 (s, ν(NO)). ^1H NMR (500 MHz, $CDCl_3$ + 3 μL of CH_3CN, 28 °C), 6.65−7.85 (m, 26 H, arom H), 2.19 (s, 3 H, MeCN), 0.62 (s, 3 H, $SiMe_3$), 0.52 ppm (s, 3 H, $SiMe_3$). ^{31}P NMR ($CDCl_3$, 121 MHz): δ −5.4 (s broad, 1 P), −2.5 (s broad, 1P); Anal. Calcd for $C_{40}H_{35}Br_2N_2O_2P_2ReSi$ (1011.77): C, 47.48; H, 3.49; N, 2.77. Found: C, 47.21; H, 3.37; N, 2.94.

[($ReBr_2$(diprpfc)(NO))$_2$] (2b). A suspension of $[ReBr_5(NO)][NEt_4]_2$ (1.000 g, 1.14 mmol) and diprpfc (1.00 g, 2.39 mmol) in absolute EtOH (10 mL) was stirred for 16 h at 80 °C. The orange precipitate was filtered off and washed with EtOH (3 × 5 mL). After it was dried in vacuo, **2b** (0.720 g, 0.45 mmol, 78%) was obtained as a yellow powder.

IR (cm^{-1}, KBr pellet): 1693 (s, ν(NO)). Anal. Calcd for $C_{44}H_{72}Br_4Fe_2N_2O_2P_4Re_2$ (1585.90): C, 33.26; H, 4.57; N, 1.76. Found: C, 33.20; H, 4.64; N, 1.82.

[$ReBrH_2$(SiEt$_3$)(NO)(P∩P)] Complexes (4a−d): Representative Procedure for 4c. An NMR tube was charged with a suspension of **1c** (10 mg, 0.01 mMol) in $HSiEt_3$ (50 μL, 0.28 mMol) and THF-d_8 (500 μL). The NMR tube was sonicated for 1 h at 50 °C before measuring the ^1H and $^{31}P\{^1H\}$ spectra of the solution. The volatiles were quickly removed in vacuo before the remaining solid was used for IR spectroscopy.

Spectroscopic data of **4a** are as follows. IR (KBr pellet, cm^{-1}): 1968 (m, broad, ν(ReH)), 1684 (s, ν(NO)). ^1H NMR (500 MHz, THF, 28 °C): δ 8.45−7.00 (m, 20 H, phenyl), 5.152 (s, 1 H, cp), 4.656 (s, 1 H, cp), 4.525 (s, 1 H, cp), 4.43−4.30 (m, 5 H, cp), 1.154 (m, 2 H, ReH), 1.18−0.54 ppm (overlapping signals of $HSiEt_3$ and $ReSiEt_3$). $^{31}P\{^1H\}$ NMR (125 MHz, THF-d_8, 28 °C): δ 3.9 ppm.

Spectroscopic data of **4b** are as follows. IR (KBr pellet, cm^{-1}): 1981 (m, broad, ν(ReH)), 1671 (s, ν(NO)). ^1H NMR (500 MHz, THF, 28 °C): δ 4.766 (s, 2 H, cp), 4.434 (s, 2 H, cp), 4.354 (s, 4 H, cp), 2.752

(m, 2 H, *i*-Pr), 2.610 (m, 2 H, *i*-Pr), 1,6−0.5 (overlapping multiplets, *i*-Pr, ReH, $ReSiEt_3$, $HSiEt_3$) ppm. $^{31}P\{^1H\}$ NMR (125 MHz, THF-d_8, 28 °C): δ 12.0 ppm.

Spectroscopic data of **4c** are as follows. IR (KBr pellet, cm^{-1}): 2004 (m, broad, ν(ReH)), 1678 (s, ν(NO)). ^1H NMR (500 MHz, THF, 28 °C): δ 6.670 (m, 3 H, phenyl), 7.50−7.25 (m, 14 H, phenyl), 7.196 (m, 3 H, phenyl), 7.075 (m, 4 H, phenyl), 6.70 (m, 3 H, phenyl), 1.17−0.51 (overlapping signals $HSiEt_3$ and $ReSiEt_3$), 0.688 ppm (m, 2 H, ReH). $^{31}P\{^1H\}$ NMR (125 MHz, THF-d8, 28 °C): δ −5.0 ppm.

Spectroscopic data of **4d** are as follows. IR (KBr pellet, cm^{-1}): 2008 (m, broad, ν(ReH)), 1683 (s, ν(NO)). ^1H NMR (500 MHz, THF, 28 °C): δ 6.648 (t, J = 9.0 Hz, 4 H, phenyl), 7.35−7.05 (m, 18 H, phenyl), 6.901 (t, J = 7.5 Hz, 2H), 6.513 (t, J = 8.0 Hz, 2 H, phenyl), 3.25−3.05 (m, 4 H, homoxantphos-CH_2CH_2), 1.17−0.51 (overlapping signals $HSiEt_3$ and $ReSiEt_3$), 0.755 ppm (m, 2 H, ReH). $^{31}P\{^1H\}$ NMR (125 MHz, THF-d_8, 28 °C): δ −0.2 ppm.

[$ReBrH_2$(diprpfc)(NO)($SiMe_3$)] (4f). A suspension of **2b** (0.105 g, 0.07 mmol) and 15% $HSiMe_3$ in THF (0.4 mL, 0.57 mmol) in THF (10 mL) was stirred for 6 h at room temperature. The resulting orange solution was filtered through a short plug of Celite and dried in vacuo to yield **4f** (0.095 g, 0.12 mmol, 92%) as a yellow powder.

IR (KBr pellet, cm^{-1}): 1974 (m, ν(ReH)), 1678 (s, ν(NO)). ^1H NMR (500 MHz, C_6D_6, 28 °C): δ 4.660 (s, 2 H, Cp), 4.190 (s, 2 H, Cp), 3.975 (s, 4 H, Cp), 2.652 (d heptet, $^3J_{HH}$ = 7 Hz, J_{PH} = 9.5, 2 H, *i*-Pr CH), 2.350 (d heptet, $^3J_{HH}$ = 7 Hz, J_{PH} = 8.5, 2 H, *i*-Pr CH), 1.839 (m, 2 H, ReH), 1.644 (dt, $^3J_{HH}$ = 7 Hz, $^3J_{PH}$ = 15 Hz, 6 H, *i*-Pr CH), 1.484 (dt, $^3J_{HH}$ = 7 Hz, $^3J_{PH}$ = 14.5 Hz, 6 H, *i*-Pr CH), 1.220 (s, 9 H, $Si(CH_3)_3$), 1.091 ppm (m, 6 H, *i*-Pr CH). $^{31}P\{^1H\}$ NMR (125 MHz, THF-d_8, 28 °C): δ 16.30 ppm. Anal. Calcd for $C_{25}H_{47}BrFeNOP_2ReSi$ (733.79). C, 38.03; H, 6.00; N, 1.77. Found: C, 37.88; H, 5.90; N, 1.71.

[$ReBrH_2$(diprpfc)(NO)($SiCl_3$)] (4g). A suspension of **1b** (0.100 g, 0.06 mmol) and $[NEt_4]Cl$ (0.250 g, 1.5 mmol) in CH_2Cl_2 (10 mL) was stirred for 2 h at 39 °C. Then $HSiCl_3$ (5 mL, 39.4 mmol) was added and stirring was continued for 2 h at 39 °C. The volatiles were removed in vacuo and the residue extracted with THF. The extract was dried in vacuo and chromatographed on a silica gel column with CH_2Cl_2 as eluent. A bright yellow fraction was collected and the solvent was removed in vacuo, yielding **4g** as bright yellow powder (0.065 g, 0.08 mmol, 66%).

IR (cm^{-1}, KBr pellet): 2001, 1938 (m, ν(ReH)), 1718 (s, ν(NO)). ^1H NMR (500 MHz, THF-d_8, 28 °C): δ 4.789 (s, 2 H, Cp), 4.560 (s, 2 H, Cp), 4.539 (s, 2 H, Cp), 4.514 (s, 2 H, Cp), 3.005 (m, 2 H, ReH), 2.759 (m, 2 H, *i*-Pr CH), 2.712 (m, 2 H, *i*-Pr CH), 1.636 (dd, $^3J_{HH}$ = 7.0 Hz, $^3J_{HP}$ = 8.5 Hz, *i*-Pr CH_3), 1.611 (dd, $^3J_{HH}$ = 7.0 Hz, $^3J_{HP}$ = 8.5 Hz, *i*-Pr CH_3), 1.310 (dd, $^3J_{HH}$ = 7.0 Hz, $^3J_{HP}$ = 7.5 Hz, *i*-Pr CH_3), 1.305 ppm (dd, $^3J_{HH}$ = 7.0 Hz, $^3J_{HP}$ = 7.5 Hz, *i*-Pr CH_3). $^{31}P\{^1H\}$ NMR (125 MHz, THF-d_8, 28 °C): δ 24.01 ppm. Anal. Calcd for $C_{22}H_{38}Cl_4FeNOP_2ReSi$ (806.44). C, 32.77; H, 4.75; N, 1.74. Found: C, 32.69; H, 4.81; N, 1.76.

■ ASSOCIATED CONTENT

Supporting Information. CIF files, text, figures, and tables giving details of the crystallographic structure determinations. This material is available free of charge via the Internet at http://pubs.acs.org.

■ AUTHOR INFORMATION

Corresponding Author
*E-mail: hberke@aci.uzh.ch.

■ ACKNOWLEDGMENT

We thank the Swiss National Science Foundation and the University of Zürich for financial support.

■ REFERENCES

(1) Jiang, Y.; Blacque, O.; Fox, T.; Frech, C., M.; Berke, H. *Chem. Eur. J.* **2009**, *15*, 2121–2128.
(2) Green, M.; L., H.; Pratt, L.; Wilkinson, G. *J. Chem. Soc.* **1958**, 3916–3922.
(3) Gusev, D.; Llamazares, A.; Artus, G.; Jacobsen, H.; Berke, H. *Organometallics* **1999**, *18*, 75–89.
(4) Chatt, J.; Coffey, S. *J. Chem. Soc. A* **1969**, 1963–1969.
(5) Luo, X. L.; Crabtree, R., H. *J. Am. Chem. Soc.* **1990**, *112*, 4813–4821.
(6) Gusev, D., G.; Nietlispack, D.; Eremenko, I., L.; Berke, H. *Inorg. Chem.* **1993**, *32*, 3628–3636.
(7) Baudry, D.; Ephritikhine, M.; Felkin, H. *J. Organomet. Chem.* **1982**, *224*, 363–376. Herrmann, W. A.; Okuda, J. *Angew. Chem.* **1986**, *98*, 1109–1111. Jones, W. D.; Maguire, J., A. *Organometallics* **1987**, *6*, 1301–1311.
(8) Mayer, J., M.; Thorn, D., L.; Tulip, T., H. *J. Am. Chem. Soc.* **1985**, *107*, 7454–7462.
(9) Blaser, H. U.; Malan, C.; Pugin, B.; Spindler, F.; Steiner, H.; Studer, M. *Adv. Synth. Catal.* **2003**, *345*, 103–151. Chen, B.; Dingerdissen, U.; Krauter, J. G.; Rotgerink, H.; Mobus, K.; Ostgard, D. J.; Panster, P.; Riermeier, T. H.; Seebald, S.; Tacke, T.; Trauthwein, H. *Appl. Catal., A* **2005**, *280* (1), 17–46.
(10) Zimmermann, S.; Sures, B. *Environ. Sci. Pollut. Res.* **2004**, *11* (3), 194–199. Schmid, M.; Zimmermann, S.; Krug, H. F.; Sures, B. *Environ. Int.* **2007**, *33*, 385–390.
(11) Garrett, C., E.; Prasad, K. *Adv. Synth. Catal.* **2004**, *346*, 889–900.
(12) Noyori, R.; Hashiguchi, S. *Acc. Chem. Res.* **1997**, *30*, 97–102.
(13) Kalck, P.; Peres, Y.; Jenck, J. *Adv. Organomet. Chem.* **1991**, *32*, 121–146.
(14) Choualeb, A.; Maccaroni, E.; Blacque, O.; Schmalle, H. W.; Berke, H. *Organometallics* **2008**, *27*, 3474–3481. Maccaroni, E.; Dong, H.; Blacque, O.; Schmalle, H., W.; Frech, C., M.; Berke, H. *J. Organomet. Chem.* **2010**, *695* (4), 487–494.
(15) Jiang, Y.; Blacque, O.; Fox, T.; Frech, C., M.; Berke, H. *Organometallics* **2009**, *28*, 5493–5504.
(16) Liu, L.; Bi, S.; Sun, M.; Yuan, X.; Zheng, N.; Li, P. *J. Organomet. Chem.* **2009**, *694*, 3343–3348.
(17) Choualeb, A.; Blacque, O.; Schmalle, H. W.; Fox, T.; Hiltebrand, T.; Berke, H. *Eur. J. Inorg. Chem.* **2007**, 5246–5261.
(18) Tolman, C. A. *J. Am. Chem. Soc.* **1970**, *92* (10), 2953–2956.
(19) Tolman, C. A. *Chem. Rev.* **1977**, *77* (3), 313–348.
(20) Casey, C. P.; Whiteker, G. T. *Isr. J. Chem.* **1990**, *30* (4), 299–304.
(21) Kranenburg, M.; van der Burgt, Y. E. M.; Kamer, P. C. J.; van Leeuwen, P. W. N. M.; Goubitz, K.; Fraanje, J. *Organometallics* **1995**, *14* (6), 3081–3089. van der Veen, L. A.; Keeven, P. H.; Schoemaker, G. C.; Reek, J. N. H.; Kamer, P. C. J.; van Leeuwen, P. W. N. M.; Lutz, M.; Spek, A. L. *Organometallics* **2000**, *19*, 872–883.
(22) Godfrey, S. M.; McAuliffe, C. A.; Mushtaq, I.; Pritchard, R. G.; Sheffield, J. M. *J. Chem. Soc., Dalton Trans.* **1998**, 3815–3818.
(23) von Zelewsky, A. Stereochemistry of coordination compounds. In *Inorganic Chemistry*; Wiley: Chichester, U.K., 1995.
(24) Chatt, J.; Duncanson, L. A. *J. Chem. Soc.* **1953**, 2939–2947.
(25) Rowland, S., R.; Taylor, R. *J. Phys. Chem.* **1996**, *100*, 7384–7391. Bondi, A. *J. Phys. Chem.* **1964**, *68*, 441–451.
(26) Crabtree, R. *Acc. Chem. Res.* **1979**, *12*, 331–337.
(27) Butler, I., R.; Cullen, W., R. *Organometallics* **1986**, *5*, 2537–2542.
(28) Gottlieb, H. E; Kotlyar, V.; Nudelman, A. *J. Org. Chem.* **1997**, *62*, 7512–7515.